

REDSHIFT DEPENDENCE OF THE COSMIC MICROWAVE BACKGROUND TEMPERATURE FROM SUNYAEV–ZELDOVICH MEASUREMENTS

G. LUZZI¹, M. SHIMON², L. LAMAGNA¹, Y. REPHAELI^{2,3}, M. DE PETRIS¹, A. CONTE¹, S. DE GREGORI¹, AND E. S. BATTISTELLI¹

¹ Department of Physics, University “La Sapienza,” P.le Aldo Moro 2, 00185, Rome, Italy

² Center for Astrophysics and Space Sciences, University of California, San Diego, 9500 Gilman Drive, La Jolla, CA 92093-0424, USA

³ School of Physics and Astronomy, Tel Aviv University, Tel Aviv 69978, Israel

Received 2009 June 12; accepted 2009 September 17; published 2009 October 19

ABSTRACT

We have determined the cosmic microwave background temperature, $T(z)$, at redshifts in the range 0.023–0.546, from multi-frequency measurements of the Sunyaev–Zeldovich (S–Z) effect toward 13 clusters. We extract the parameter α in the redshift scaling $T(z) = T_0(1+z)^{1-\alpha}$, which contrasts the prediction of the standard model ($\alpha = 0$) with that in non-adiabatic evolution conjectured in some alternative cosmological models. The statistical analysis is based on two main approaches: using ratios of the S–Z intensity change, ΔI , thus taking advantage of the weak dependence of the ratios on intracluster gas properties, and using directly the ΔI measurements. In the former method, dependence on the Thomson optical depth and gas temperature is only second order in these quantities. In the second method, we marginalize over these quantities which appear to first order in the intensity change. The marginalization itself is done in two ways—by direct integrations and by a Monte Carlo Markov chain approach. Employing these different methods we obtain two sets of results that are consistent with $\alpha = 0$, in agreement with the prediction of the standard model.

Key words: cosmic microwave background – cosmology: observations – galaxies: clusters: individual (A1656, A2204, A1689, A520, A2163, A773, A2390, A1835, A697, ZW3146, RXJ1347, CL0016+16, MS0451–0305)

Online-only material: color figure

1. INTRODUCTION

The variation of the cosmic microwave background (CMB) temperature with redshift is a basic relation which in adiabatically evolving cosmological models is $T(z) = T_0(1+z)$, normalized to the *COBE*/FIRAS value at the present epoch, $T_0 = 2.725 \pm 0.002$ K (Mather et al. 1999). In light of the fundamental role the CMB plays in cosmology, and given our detailed knowledge of its spatial structure, the lack of precise observational confirmation of this important relation is rather surprising. Further motivation to measure $T(z)$ is provided by the prediction of different nonlinear redshift scaling law in alternative cosmological models (e.g., Overduin & Cooperstock 1998; Matyjasek 1995; Puy 2004). In particular, we consider here the scaling law proposed by Lima et al. (2000), $T(z) = T_0(1+z)^{1-\alpha}$, with α being a free (constant) parameter; this scaling is presumed to be a consequence of photon number and radiation entropy non-conservation.

The $T(z)$ dependence has traditionally been tested by measurements of quasar absorption spectra which include fine-structure lines from interstellar atoms and ions (e.g., LoSecco et al. 2001). Using this method the CMB temperature was measured to a maximum redshift of 3.025, at which $T \simeq 12.6_{-3.2}^{+1.7}$ K was determined from an analysis of the C II fine-structure lines in the damped $L\gamma_\alpha$ system toward the quasar Q0347–3819 (Molaro et al. 2002). The fact that the CMB is not the only radiation field populating the energy levels (from which the transitions occur), and lack of detailed knowledge of the physical conditions in the absorbing clouds—is a major source of systematic uncertainty (e.g., Combes & Wiklind 1999). A strong limit on α was deduced (Opher & Pelison 2005) using CMB and galaxy distribution data. However, this method cannot be used to determine the $T(z)$ scaling.

The possibility of determining $T(z)$ from measurements of the Sunyaev–Zeldovich (S–Z) effect had been suggested long ago (Fabbri et al. 1978; Rephaeli 1980). The effect—Compton scattering of the CMB by hot intracluster (IC) gas—is a small change of the CMB spectral intensity, ΔI , which depends on the integrated IC gas pressure along the line of sight (los) to the cluster. The steep frequency dependence of the change in the CMB spectral intensity, ΔI , due to the S–Z effect allows the CMB temperature to be estimated at the redshift of the cluster. Since the ratio of the values of ΔI measured at two frequencies is essentially independent of the cluster properties, the value of the temperature at the cluster redshift can be deduced directly from this ratio (Rephaeli 1980). The much improved capability of precise multi-frequency measurements of the effect enhances interest in this method to measure $T(z)$ in nearby and moderately distant clusters.

The first attempt to determine $T(z)$ from an analysis of multifrequency S–Z measurements in the Coma and A2163 clusters of galaxies was reported in Battistelli et al. (2002). Preliminary results from an analysis of a larger sample of clusters, with $z = 0.023$ –0.546, was presented in De Gregori et al. (2008). In this paper, we report the final results from the current cluster sample carrying out a significantly expanded statistical data analysis. The statistical analysis is based on both ratios of ΔI , which are weakly dependent on the cluster properties, as well as the values of the individual ΔI whose dependence on cluster properties is marginalized over (also) the Thomson optical depth. We discuss the consistency between these two analysis methods.

In Section 2, we outline the basic methods used to determine $T(z)$. Data analysis and the results for α are presented in Section 3. We end with a brief summary in Section 4.

2. METHOD

Compton scattering of the CMB in a cluster causes a change of intensity that can be written as

$$\Delta I = \frac{2k^3 T^3}{h^2 c^2} \frac{x^4 e^x}{(e^x - 1)^2} \int d\tau [\theta f_1(x) - \beta + R(x, \theta, \beta)], \quad (1)$$

where $x \equiv hv/kT$ is the dimensionless frequency, $\theta = kT_e/mc^2$ is the electron temperature in units of the electron rest energy, and β is the los component of the cluster velocity (divided by c) in the CMB frame. The integral is over the Thomson optical depth, τ . Both the thermal (Sunyaev & Zel'dovich 1972) and kinematic (Sunyaev & Zel'dovich 1980) components of the effect are included in Equation (1) in the first two terms, and in the function $R(x, \theta, \beta)$. This latter term is the relativistic correction (Rephaeli 1995) to the non-relativistic expressions for the thermal and kinematic components. An analytic approximation (which is sufficiently exact even close to the crossover frequency) can be written in the form

$$R(x, \theta, \beta) \simeq \theta^2 [f_2(x) + \theta f_3(x) + \theta^2 f_4(x) + \theta^3 f_5(x)] - \beta \theta [g_1(x) + \theta g_2(x)] + \beta^2 [1 + \theta g_3(x)]. \quad (2)$$

The spectral functions f_i and g_i are specified in Shimon & Rephaeli (2004); see also Itoh et al. (2002).

With $T(z) = T(0)(1+z)^{(1-\alpha)}$ and $v = v_0(1+z)$, the non-dimensional frequency depends on redshift if $\alpha \neq 0$, $x = x_0(1+z)^\alpha$, with $x_0 = hv_0/kT(0)$. The steep frequency dependence of the change in the CMB spectral intensity allows the CMB temperature to be estimated at the redshift of the cluster. In the non-relativistic limit ΔI depends linearly on the Comptonization parameter, $y = \int \theta d\tau$, which includes all dependence on IC gas properties. A ratio of values of ΔI at two frequencies is then essentially independent of the cluster properties. In the more general case, the first term in the square parentheses in Equation (1) still dominates over the other two, except near the crossover frequency, where the sum of the temperature-dependent terms vanishes. For values of x outside some range (roughly, $3.5 < x < 4.5$), the dependence of ΔI on β is very weak since the observed temperature range in clusters corresponds to $0.006 < \theta < 0.03$, whereas typically $\beta < 0.002$. Therefore, data points at or near the crossover frequency are noise dominated, and thus carry relatively low statistical weight in the likelihood function we construct for α or $T(z)$. Nevertheless, we include these points in our analysis.

3. DATA ANALYSIS

We analyzed results of multi-frequency S–Z measurements toward 13 clusters spanning the redshift range 0.023–0.550. The data set includes measurements with the Berkeley-Illinois-Maryland-Association (BIMA), Owens Valley Radio Observatory (OVRO), Sunyaev-Zel'dovich Infrared Experiment (SuZIE-II), Submillimeter Common-User Bolometric Array (SCUBA), and Millimeter and Infrared TestaGrigia Observatory (MITO) telescopes, as well as gas temperatures determined from X-ray measurements. We assumed a Gaussian profile for the spectral bands of each experiment. In order to evaluate systematics induced by different spectral efficiencies of the bands, we repeated the analysis with squared profiles. The error contribution is negligible as compared with uncertainties in values of the central frequency and bandwidth. The clusters, redshifts, and gas temperatures are listed in Table 1, and the S–Z data

Table 1
Cluster Redshift and Gas Temperatures

Cluster	z	kT_e^a (keV)
A1656	0.023	8.25 ± 0.10^b
A2204	0.152	11.53 ± 2.80
A1689	0.183	9.59 ± 2.80
A520	0.200	8.33 ± 0.76
A2163	0.202	16.18 ± 3.86
A773	0.216	6.62 ± 1.30
A2390	0.232	10.13 ± 1.22
A1835	0.252	13.45 ± 4.02
A697	0.282	10.60 ± 1.13
ZW3146	0.291	8.12 ± 1.00
RXJ1347	0.451	13.69 ± 2.64
CL0016+16	0.546	10.10 ± 2.57
MS0451–0305	0.550	10.68 ± 2.93

Notes.

^a Bonamente et al. (2006).

^b Arnaud et al. (2001).

are in Table 2. In the analysis we allowed for calibration uncertainty, considered as an uncertain scale factor, which was modeled as a Gaussian with mean 1 and 10% standard deviation.⁴ This is an adequate approximation given the relatively narrow widths of the respective Gaussian distributions. For the radial component of the cluster peculiar velocities we assume a universal vanishing mean with a 1000 km s^{−1} standard deviation.

The calculation begins with convolution of $\Delta I(\nu)$ with the detector Gaussian spectral response function with width σ_{ν_0} ,

$$\Delta I(\nu_0) \equiv \frac{1}{\sqrt{2\pi}\sigma_{\nu_0}} \int_{\nu=0}^{\infty} \Delta I(\nu) e^{-\frac{(\nu-\nu_0)^2}{2\sigma_{\nu_0}^2}} d\nu, \quad (3)$$

using the approximate analytic expression for (the relativistically correct) $\Delta I(\nu)$ derived by Shimon & Rephaeli (2004). Integration by parts then yielded an analytic approximation to the frequency-convolved $\Delta I(\nu)$, accurate to order $(\sigma_{\nu_0}/\nu)^4$. The sole purpose of deriving the latter analytic (rather cumbersome) approximations (which are not specified here) was to enable a faster convolution of the theoretical expression for $\Delta I(\nu)$ with the detector Gaussian spectral response.

The probability of measuring an intensity change $\Delta I_{\text{obs}}(\nu_j)$ at frequency ν_j toward a cluster at redshift z_i , with velocity parameter β_i , gas parameters τ_i, θ_i , and model parameter α is

$$P(\tau_i, \theta_i, \beta_i; z_i, \alpha)$$

$$\propto \exp \left\{ - \sum_j \frac{[\Delta I(\tau_i, \theta_i, \beta_i, \nu_j; \alpha) - \Delta I_{\text{obs}}(\nu_j)]^2}{2\sigma_I^2(\nu_j)} \right\}, \quad (4)$$

where ΔI is the result of convolution of the theoretically predicted intensity change with the spectral response function (calculated using Equation (3)), and $\sigma_I(\nu_j)$ is measurement error standard deviation.

The CMB temperature at the redshift of each cluster was first extracted by performing statistical analysis on the ratios $r_{ij} = \Delta T(\nu_i)/\Delta T(\nu_j)$ ($\Delta T(\nu_i)$ is the observed thermodynamic

⁴ The calibration errors for the experiments considered are at a maximum level of 10%, based on observations of the brightness of planets. We have adopted a conservative approach in assuming maximum errors in order not to be biased by different calibration procedures of different experiments.

Table 2
SZE Measurements of 13 Clusters by Different Experiments Expressed in Central Thermodynamic Temperature

Cluster	OVRO+BIMA ^a		SuZIE II ^b			SCUBA ^c
	$\Delta T_{30\text{ GHz}}$ (mK)	$\Delta T_{145\text{ GHz}}$ (mK)	$\Delta T_{221\text{ GHz}}$ (mK)	$\Delta T_{273\text{ GHz}}$ (mK)	$\Delta T_{355\text{ GHz}}$ (mK)	$\Delta T_{353\text{ GHz}}$ (mK)
A520	-0.66 ± 0.09^d	-0.44 ± 0.13	0.14 ± 0.14	...	1.78 ± 0.41	2.60 ± 0.57
A697	-1.22 ± 0.12	-0.93 ± 0.13	0.41 ± 0.16	...	2.80 ± 0.62	...
A773	-1.08 ± 0.11	-0.91 ± 0.16	0.04 ± 0.25	...	2.40 ± 0.89	2.7 ± 2.0
A1689	-2.06 ± 0.17	2.93 ± 0.40
A1835	-2.90 ± 0.21	-1.74 ± 0.26	0.14 ± 0.41	1.73 ± 0.59
A2204	-3.22 ± 0.32	-0.65 ± 0.10	0.21 ± 0.10	...	1.85 ± 0.44	...
A2390	...	-0.91 ± 0.10	-0.10 ± 0.17	...	1.23 ± 0.34	2.40 ± 0.44
CL0016+16	-1.44 ± 0.09	-0.57 ± 0.23	0.66 ± 0.46	1.82 ± 0.68	...	1.96 ± 0.64
MS0451-03	-1.48 ± 0.09	-0.779 ± 0.065	-0.21 ± 0.10	0.91 ± 0.66	1.16 ± 0.34	...
RXJ1347	-5.15 ± 0.60	-3.22 ± 0.39	-0.10 ± 0.39	...	6.2 ± 1.5	5.36 ± 0.54
ZW3146	-2.02 ± 0.25	-1.56 ± 0.39	-0.25 ± 0.48	...	3.1 ± 1.3	...
	OVRO ^d		MITO ^e		SCUBA ^c	
Cluster	$\Delta T_{32\text{ GHz}}$ (mK)	$\Delta T_{143\text{ GHz}}$ (mK)	$\Delta T_{214\text{ GHz}}$ (mK)	$\Delta T_{272\text{ GHz}}$ (mK)		$\Delta T_{353\text{ GHz}}$ (mK)
A1656	-0.520 ± 0.093	-0.179 ± 0.037	0.033 ± 0.080	0.170 ± 0.034		...
	OVRO+BIMA ^a		SuZIE I ^f		SCUBA ^c	
Cluster	$\Delta T_{30\text{ GHz}}$ (mK)	$\Delta T_{142\text{ GHz}}$ (mK)	$\Delta T_{217\text{ GHz}}$ (mK)	$\Delta T_{268\text{ GHz}}$ (mK)		$\Delta T_{353\text{ GHz}}$ (mK)
A2163	-1.89 ± 0.17	-1.011 ± 0.098	-0.21 ± 0.16	0.66 ± 0.24		...

Notes.

^a Bonamente et al. (2006).

^b Benson et al. (2003, 2004).

^c Zemcov et al. (2007).

^d Herbig et al. (1995); Mason et al. (2001).

^e De Petris et al. (2002); Savini et al. (2003).

^f Holzapfel et al. (1997).

temperatures in the i th photometric band) marginalizing over θ and β —the original (hereafter) RI approach—and by using each of these separately and marginalizing also over τ , θ and β —the DI approach.⁵ Assuming the S–Z data are Gaussianly distributed allows us to construct the relevant single-cluster and multiple-cluster likelihood functions. We note that the high-dimensionality of the marginalization, over the full parameter space, including also the calibration uncertainty (see Section 3.1) can potentially be a source for large numerical errors. We therefore employed two separate pipelines in the DI analysis—a direct numerical integration and Monte Carlo Markov chain (MCMC) sampling. After proper treatment of the systematics the different methods give consistent results.

3.1. Likelihood of Intensity Ratios

The RI approach—first employed in our previous work (Battistelli et al. 2002)—is based on the use of the likelihood function of intensity ratios, thereby removing (to first order) dependence on the Comptonization parameter (Rephaeli 1980). By doing so we largely avoid the need to account for modeling uncertainties in the determination of the gas density and temperature profiles (from X-ray surface brightness and spectral measurements). Dependence on the measured gas temperatures, T_e , is also largely removed in the leading term, although T_e is still needed to calculate the relativistic correction which includes

second-order terms in T_e . Measurements at the crossover frequency were not included in the analysis due to the inherent problematics associated with inclusion of very weak signals in the likelihood function (e.g., “Cauchy tail,” bimodality, etc.), which are expected to be dominated by instrumental noise and systematic uncertainties, so their relative weight in the likelihood function would be negligible.

The distribution of ratios may have complicated features, but if carefully applied can be a very powerful tool due to the reduced number of essential parameters in the problem. In our case the distribution of ratios of temperature changes is manifestly non-Gaussian, but we are interested in constraining the CMB temperature (or the parameter α) rather than ΔT itself. The distribution is expected to be normal when the cluster sample is large. As shown in the Appendix, this approach has the unwanted feature that the expectation value of the ratio is biased to a degree which is of $O((\Delta T/T)^2)$, but in the limit of very precise measurements the fractional error decreases as does the degree of bias. This follows from the fact that a uni-modal distribution function behaves as a Gaussian sufficiently close to its peak, and if measurement errors are sufficiently small the function is sharply peaked. In other words, when the function is highly concentrated near the peak, any value of the parameter (for which the distribution function does not vanish) is in the “Gaussian-regime.” This guarantees that the ratio distribution is an unbiased Gaussian. However, for the small number of clusters in our present sample, and the low quality of some of the measurements, our results are still affected by this bias, but at a level smaller than the statistical uncertainty. The situation will improve substantially in the near future, when planned surveys

⁵ Note that for marginalizing over a range of gas temperatures we have determined this range by using a beta profile for the gas density. The modeling uncertainty due to the use of this profile is negligible.

with PLANCK and other S–Z projects will provide a very large sample of clusters. A more complete discussion of the ratio approach is given in the [Appendix](#).

The joint distribution function is derived from a set of n S–Z measurements (at n different frequency bands, excluding the crossover frequency) of a given cluster. In doing so we choose the S–Z data point with the smallest fractional error to be in the denominator of the $n - 1$ ratios so as to minimize the bias (the [Appendix](#)). We construct the likelihood function of the simultaneously calculated $n - 1$ ratios for a given frequency (in the denominator) obtaining a single likelihood function per cluster.

The likelihood function that encapsulates the multi-cluster information is defined as

$$L(\alpha) \equiv \prod_i L(\theta_i, \beta_i, C; \alpha) \quad (5)$$

where the index i runs over all clusters in the sample. In the following, we marginalize over θ_i , β_i , and calibration uncertainty, denoted here by C . In the limit of sufficiently large data set, the joint likelihood function is Gaussian in α by virtue of the central limit theorem and in accord with the reasoning we specified above. The average gas temperatures and their errors, as obtained from X-ray observations, are summarized in [Table 1](#). The smaller (than thermal) kinematic component vanishes to first order (due to motion either toward or away from the observer).

3.2. The DI Approach

As noted, we carried out another independent analysis based on using the measured values of ΔI themselves, rather than their ratios. This second approach was implemented in two separate and very different treatments. The first consisted of the construction of a likelihood function that incorporates the multi-cluster information, with direct numerical two-dimensional integrations involved in the marginalization over τ , θ , β , and C (the integration over β and C is carried out analytically after Taylor expanding the integrand in powers of β and C)

$$L(\alpha) \equiv \prod_i L(\tau_i, \theta_i, \beta_i, C; \alpha). \quad (6)$$

For τ we use a flat (positive definite) prior; for the other parameter priors are chosen as in the RI approach (see [Section 3](#)).

The second independent treatment is based on MCMC sampling, which is very commonly used in a wide class of problems, where complex dependences between the parameters greatly impact the likelihood function, so that direct integrations could be quite tedious and prone to numerical instabilities (e.g., [Lewis & Bridle 2002](#); [Verde 2007](#)). In this treatment, we construct a single likelihood for each cluster, in order to get directly $T(z)$ at the cluster redshift, and also to check parameter degeneracies.

The MCMC method constitutes a random sequence of realizations of the fit parameters which—when properly sampled in parameter space—tends to reproduce the posterior distribution for all the parameters. The technique is easily implemented into an iterative code that draws candidate sets of fitting parameters of chain elements from a given proposal distribution, and inserts the candidates into the chain if some proper statistical criterion is met. The sampling approach we used is the one proposed by Metropolis and Hastings ([Metropolis et al. 1953](#); [Hastings 1970](#)). According to this scheme, each candidate set of parameters ϑ_i is drawn from a Gaussian centered over the previously

Table 3
 $T(z)$ Values as Estimated for Each Cluster

Cluster	$T(z)$ (K)
A1656	2.72 ± 0.10
A2204	2.90 ± 0.17
A1689	2.95 ± 0.27
A520	2.74 ± 0.28
A2163	3.36 ± 0.20
A773	3.85 ± 0.64
A2390	3.51 ± 0.25
A1835	3.39 ± 0.26
A697	3.22 ± 0.26
ZW3146	4.05 ± 0.66
RXJ1347	3.97 ± 0.19
CL0016+16	3.69 ± 0.37
MS0451	4.59 ± 0.36

Note. We report expected values and standard deviations.

accepted chain element ϑ_{i-1} . The width of the proposal distribution is a critical parameter of the code which determines the efficiency of the sampling algorithm (i.e., the capability to sample from the multi-parameter posterior distribution in a given number of realizations, or acceptance rate) and its ability to explore the full domain of the fitting parameters. Different test runs of the MCMC code were needed to find the best tradeoff between acceptance rate and accuracy of the fit for given chain lengths, by adjusting the width of the proposal distributions. In the final configuration, the code was able to reconstruct the posteriors with 5%–10% acceptance rate and sufficient samplings of the parameter space were achieved in less than 10^6 samplings. Convergence of the MCMC runs was also tested through the Gelman–Rubin test ([Gelman et al. 1992](#)) which not only tests convergence but can also diagnose poor mixing. We have verified that the results are independent of the starting point in parameter space by performing multiple shorter runs of the code and confirming the statistical consistency of the results of the single runs. Undersampling of the final chains was performed to reduce the self-correlation which is naturally induced in a sampled Markov chain, and may therefore affect the estimate of sample variances for the different parameters. Once we have the posteriors for the various parameters we can characterize the distributions in terms of the quantities of interest: expected value, mode, standard uncertainty, and probability intervals.

The above analysis has been performed for each cluster to derive $T(z)$. We present the results in terms of $T(z)$ in [Table 3](#), where we give expected values and standard deviations. Note that $T(z)$ at the cluster redshift is independent of the particular scaling assumed for the temperature (i.e., the Lima model in this case); the only assumption made is that the frequency obeys the standard scaling, $\nu(z) = \nu_0(1+z)$ is valid. Rather, the α value is strictly related to the specific model under consideration.

By studying the correlations between the variables, we checked that the main degeneracies are between $T(z)$ and τ , and $T(z)$ and β . In particular, given the actual level of low-precision S–Z measurements, only the correlation between $T(z)$ and β is always evident. We verified this behavior by simulating a data set for a single cluster. We checked that, in order to reduce the impact of the degeneracy between $T(z)$ and β and then to reduce the uncertainty in the determination of $T(z)$, better knowledge of the peculiar velocity is required (see [Figure 1](#)). We used

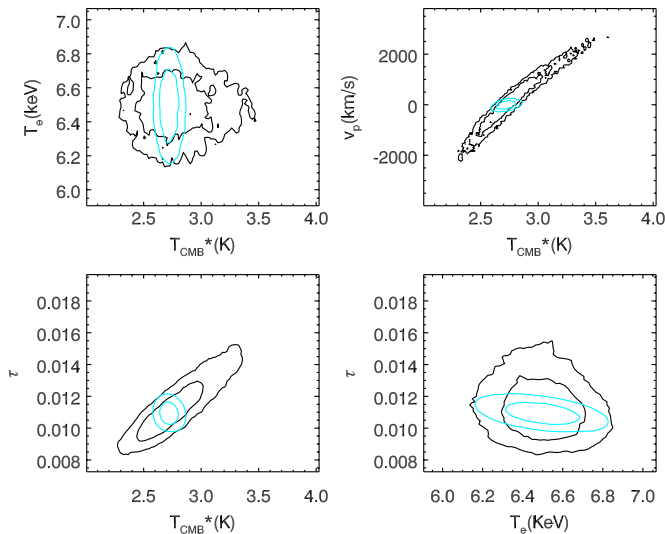


Figure 1. Parameter correlations for a simulated cluster: the contours show the 68% and 95% confidence limits from the marginalized distributions. Black contours are obtained allowing for a peculiar velocity prior with vanishing mean and standard deviation 1000 km s^{-1} ; light gray (cyan in the electronic edition) contours are obtained allowing for a peculiar velocity prior with vanishing mean and standard deviation 100 km s^{-1} . $T_{\text{CMB}}^* = T(z)/(1+z)$.

(A color version of this figure is available in the online journal.)

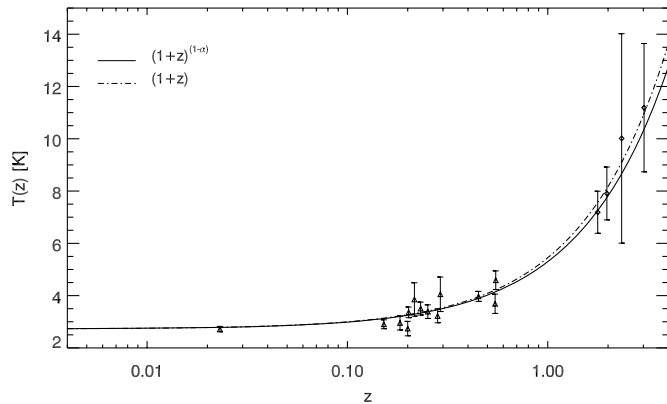


Figure 2. $T(z)$ as deduced from S–Z spectra from complete data set of clusters (Δ) together with results deduced from line transition observations (\diamond): (Cui et al. 2005; Ge et al. 1997; Srikanand et al. 2000; Molaro et al. 2002). The solid line is the best fit to the Lima scaling. The dot-dashed line is the standard scaling.

two different priors for the peculiar velocity: one Gaussian with vanishing mean and standard deviation 1000 km s^{-1} and the other Gaussian with vanishing mean and standard deviation 100 km s^{-1} .

To obtain α we have performed a fit of the $T(z)$ data points. Of course, since the distributions of $T(z)$ for individual clusters are in general slightly non-Gaussian and in addition they are frequently skewed, performing a best fit as if they were Gaussian introduces a bias in the result. Nevertheless we tested that it is a good first approximation. The prior for α is flat in the range $\alpha \in [0, 1]$, to account for the theoretical constraints of the model (Lima et al. 2000).

3.3. Results

To obtain the results we report below we assumed the flat prior $\alpha \in [0, 1]$. Employing the RI approach we deduce the most probable value $\alpha = 0.024^{+0.068}_{-0.024}$; all errors in this section are at 68% confidence. As discussed earlier, the use of intensity ratios necessarily introduces bias in the inferred parameter, although

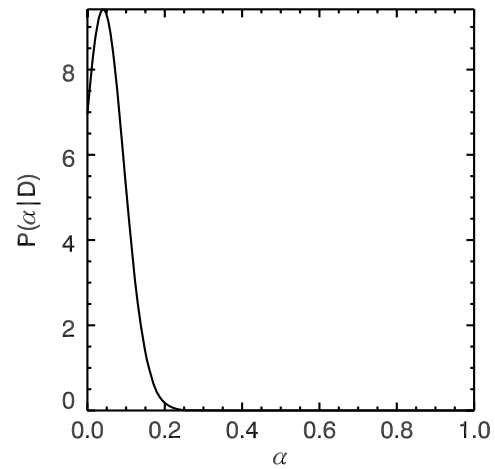


Figure 3. Posterior of the α parameter, as obtained by performing a fit of the $T(z)$ data points.

we attempted to minimize the bias by selecting the measurement with the smallest fractional error to be in the denominator of the ratios for each cluster. The more precise the measurements, the weaker is this bias. To estimate the bias in this result we repeated the calculation with observational errors in values of ΔI (used in the denominators) reduced to very small (relative) levels, thereby isolating the impact of this systematic bias. Doing so yields $\alpha = 0.038^{+0.057}_{-0.038}$. Thus, when compared with the value deduced from the actual data, $\alpha = 0.024^{+0.068}_{-0.024}$, a bias level of ~ -0.014 is indeed a relatively small fraction of the statistical uncertainty, ~ 0.057 .

The analysis was repeated employing the DI approach, adopting a flat τ prior in the interval $[0, 0.05]$. In the first direct three-dimensional integrations treatment we obtain $\alpha = 0.026^{+0.033}_{-0.026}$. The final alpha value we get by fitting the $T(z)$ data points obtained with the MCMC treatment is $\alpha = 0.062^{+0.055}_{-0.062}$. In order to check the efficiency of this method we have also considered the $T(z)$ as deduced from line transitions observations (mainly estimated by UV observations of interstellar clouds; see Figure 2). The improvement on the constraints on α is not substantial in spite of the wider redshift range (as compared to the S–Z data). The final alpha value we get by fitting the $T(z)$ data points is $\alpha = 0.041^{+0.038}_{-0.041}$. Due to the shape of the posterior (see Figure 3) as a consequence of the strong prior on α , it is more meaningful to present this result as just an upper limit, i.e., $\alpha \leq 0.079$ at 68% probability level.

Our three different treatments yield consistent results. More important, no significant evidence is found for a deviation from the redshift dependence of the CMB temperature predicted in the standard model.

In principle, the intensity-ratio approach to determine $T(z)$ would seem preferable over the DI method since dependence on τ is only second order, as compared with first-order linear dependence on this quantity, which therefore needs to be marginalized over in the DI method. This is so even if the former method is somewhat biased due to the arbitrariness in selecting the intensity change used in the denominator of the intensity ratios. Our RI upper limit, $\alpha \leq 0.092$ at the 68% confidence level, is weaker than that obtained in the DI analysis, 0.059; this reflects the fact that the 68% confidence region is wider than the usual 1σ uncertainty region when the distribution is non-Gaussian, such as the one we get with the RI approach. With more precise measurements, or—equivalently—a larger number of clusters, the distribution of ratios would approach a Gaussian

and would therefore be less affected by this bias. Ongoing and near future surveys, including those planned with the Atacama Cosmology Telescope (ACT), Atacama Pathfinder Experiment–Sunyaev-Zel’dovich (APEX-SZ), South Pole Telescope (SPT), and Planck, as well as detailed S–Z mapping of a sample of nearby clusters with the Multi Array of Detectors (MAD) (Lamagna et al. 2002) and balloon-borne OLIMPO (Masi et al. 2003) experiments, will provide much more precise and uniform data sets that will largely remove the bias in the RI approach. While there is no such bias in the DI approach, the marginalization over values of τ lowers the usefulness of this approach. On the other hand, spatially resolved spectroscopic observations of galaxy clusters (as proposed with the SAGACE satellite, a small mission project approved for Phase A by the Italian Space Agency) would allow for breaking the degeneracy between $T(z)$ and cluster parameters.

4. SUMMARY

By adopting a more general redshift scaling law that includes the prediction of the standard model when $\alpha = 0$, we are able to test both adiabatic and non-adiabatic models. While we obtain somewhat different results for α in the above three treatments, the degree of overlap of the respective uncertainty intervals implies that these values are statistically consistent. Already with the current sample of 13 clusters with medium-quality S–Z data, we are able to verify the standard scaling law at a good level of precision. More precise measurements of the $T(z)$ scaling law could possibly have interesting ramifications on setting constraints on the variation of fundamental constants over cosmological time.

We thank G. D’Agostini for useful discussions and the referee for helpful suggestions. M.S. gratefully acknowledges useful discussions with Ran Shimon. This work has been supported in part by MIUR/PRIN 2006 (prot. 2006020237) and University of Rome, La Sapienza (Ateneo prot. C26A0647AJ).

APPENDIX RATIO DISTRIBUTION

We briefly summarize some of the basic elements of the theory of ratio distributions employed in this work. If two variables x and y are drawn from distribution functions $S(x)$ and $T(y)$, respectively, then the probability that their ratio is in the interval $[r, r + dr]$ is

$$\tilde{P}(r < x/y < r + dr) = \int_{x=-\infty}^{\infty} \int_{y=r x}^{(r+dr)x} S(x)T(y)dx dy, \quad (\text{A1})$$

which can be shown to imply that

$$P(r) = \int_{-\infty}^{\infty} |x|S(x)T(rx)dx, \quad (\text{A2})$$

where in the last step we took the absolute value of the Jacobian so that the distribution function is non-negative. For Gaussian distributions S and T and finite r , this integral can be carried out analytically.

In the case of three independent, Gaussianly distributed, data points x, y, z , and considering the two ratios $r_1 = y/x$, and $r_2 = z/x$, where $r_1 = R_1(x, y)$ and $r_2 = R_2(x, z)$, the joint

density function $P(r_1, r_2)$ is

$$P(r_1, r_2) = \int \delta[r_1 - R_1(x, y)]\delta[r_2 - R_2(x, z)]f(x, y, z)dx dy dz, \quad (\text{A3})$$

where $f(x, y, z) = S(x)T(y)U(z)$ because data are independent by definition, and which once integrated, after employing $y = r_1 x$ and $z = r_2 x$, gives

$$P(r_1, r_2) \propto \int x^2 e^{-\frac{(x-\rho_1)^2}{2\sigma_1^2}} e^{-\frac{(r_1 x - \rho_2)^2}{2\sigma_2^2}} e^{-\frac{(r_2 x - \rho_3)^2}{2\sigma_3^2}} dx \quad (\text{A4})$$

(see, for example, D’Agostini 2003b).

In the case of n ratios of Gaussianly distributed $n + 1$ data-points we similarly obtain the probability for the nontrivial n ratios (in addition to the ratio r_0 which equals unity) to be simultaneously r_1, r_2, \dots, r_n

$$P(r_1, r_2, \dots, r_n; \theta, \beta_r; \alpha) \propto \int_{x=-\infty}^{\infty} dx \cdot |x|^n \times \exp \left[-\sum_{i=1}^{n+1} \frac{(x r_{i-1} - \rho_i)^2}{2\sigma_i^2} \right], \quad (\text{A5})$$

where ρ_i and σ_i are the expectation values and widths of the individual Gaussians. In our case (Table 2) n can be either 1, 2, or 3. We carried out these one-dimensional integrations numerically. In practice, the ratios r_i are the theoretical ratios of SZ observations at the various frequency bands which are functions of the gas temperatures θ and cluster peculiar velocities β_r , as well as the CMB temperature or α . The values ρ_i are measured with errors σ_i (Table 2). The next step is to marginalize Equation (A5) over the gas temperature θ and cluster velocity β_r .

A generic problem of ratio distributions is their inherent bias, which can be illustrated as follows. Assume two measurements ρ_1 and ρ_2 with Gaussian errors σ_1 and σ_2 , respectively. The probability function for the ratio r is

$$P(r) = \frac{1}{2\pi\sigma_1\sigma_2} \int_{x=-\infty}^{\infty} x e^{-\frac{(x-\rho_1)^2}{2\sigma_1^2}} e^{-\frac{(xr-\rho_2)^2}{2\sigma_2^2}} dx. \quad (\text{A6})$$

It can be easily verified that this probability function is indeed normalized, $\int_{-\infty}^{\infty} P(r)dr = 1$. Similarly, we can calculate the expectation of the ratio r ; $\langle r \rangle = \int_{-\infty}^{\infty} P(r)rdr$. A change of variables leads to

$$\langle r \rangle = \frac{1}{2\pi\sigma_1\sigma_2} \int_{-\infty}^{\infty} \frac{dx}{x} e^{-\frac{(x-\rho_1)^2}{2\sigma_1^2}} \int_{-\infty}^{\infty} z dz e^{-\frac{(z-\rho_2)^2}{2\sigma_2^2}}. \quad (\text{A7})$$

The second integral can be readily calculated and yields $\sigma_2\rho_2\sqrt{2\pi}$, and the first integral is

$$\int_{-\infty}^{\infty} \frac{dx}{x} e^{-\frac{(x-\rho_1)^2}{2\sigma_1^2}} = \frac{1}{\rho_1} \int_{-\infty}^{\infty} \frac{dx}{1 + \frac{x}{\rho_1}} e^{-\frac{x^2}{2\sigma_1^2}}. \quad (\text{A8})$$

Assuming that the measurement at the denominator of the ratio is very accurate, i.e., that $\sigma_1 \ll \rho_1$, the denominator in the integral can be expanded in powers of $\frac{x}{\rho_1}$, and the integration is then carried out term by term. The leading order expectation value for the ratio is then

$$\langle r \rangle = \frac{\rho_2}{\rho_1} \left[1 + \frac{1}{2} \left(\frac{\sigma_1}{\rho_1} \right)^2 + O \left(\left(\frac{\sigma_1}{\rho_1} \right)^4 \right) \right]. \quad (\text{A9})$$

This demonstrates the bias in ratio distributions; it is dominated by the error of the denominator and therefore we choose in all our calculations the denominator to be the measurement with the smallest fractional error as to minimize the bias. In higher dimensional distribution functions the definition of the bias is not unique and therefore cannot be unambiguously calculated and corrected for. Note, also, that the bias is in the expectation value of the ratio of SZ temperatures, and not directly in α . The exact change in α as a result of this bias is difficult to predict a priori, but for high sensitivity measurements with large samples of clusters the effective fractional error drops significantly, and the bias in α is much weaker. As in the DI method our likelihood function is obviously non-Gaussian in α and we define the average α as the median value of that distribution.

REFERENCES

- Arnaud, M., et al. 2001, *A&A*, **365**, L67
 Battistelli, E. S., et al. 2002, *ApJ*, **580**, L101
 Benson, B. A., Church, S. E., Ade, P. A. R., Bock, J. J., Ganga, K. M., Henson, C. N., & Thompson, K. L. 2004, *ApJ*, **617**, 829
 Benson, B. A., et al. 2003, *ApJ*, **592**, 674
 Bonamente, M., Joy, M. K., LaRoque, S. J., Carlstrom, J. E., Reese, E. D., & Dawson, K. S. 2006, *ApJ*, **647**, 25
 Combes, F., & Wiklind, T. 1999, in ASP Conf. Ser. 156, Highly Redshifted Radio Lines, ed. C. L. Carilli, S. J. E. Radford, K. M. Metten, & G. I. Langston (San Francisco, CA: ASP), 210
 Cui, J., Bechtold, J., Ge, J., & Meyer, D. M. 2005, *ApJ*, **633**, 649
 D'Agostini, G. 2003b, Bayesian Reasoning in Data Analysis—A Critical Introduction (Singapore: World Scientific)
 De Gregori, S., Conte, A., De Petris, M., Lamagna, L., Luzzi, G., Battistelli, E. S., & Savini, G. 2008, *Il Nuovo Cimento*, **122**, 9
 De Petris, M., et al. 2002, *ApJ*, **574**, L119
 Fabbri, R., Melchiorri, F., & Natale, V. 1978, *Astrophys. Space Sci.*, **59**, 223
 Ge, J., Bechtold, J., & Black, J. H. 1997, *ApJ*, **474**, 67
 Gelman, A., & Rubin, D. 1992, *Stat. Sci.*, **7**, 457
 Hastings, W. K. 1970, *Biometrika*, **57**, 97
 Herbig, T., Lawrence, C. R., & Readhead, A. C. S. 1995, *ApJ*, **449**, 5
 Holzapfel, W. L., Wilbanks, T. M., Ade, P. A. R., Church, S. E., Fischer, M. L., Mauskopf, P. D., Osgood, D. E., & Lange, A. E. 1997, *ApJ*, **479**, 17
 Itoh, N., Sakamoto, T., Kusano, S., Kawana, Y., & Nozawa, S. 2002, *A&A*, **382**, 722
 Lamagna, L., De Petris, M., Melchiorri, F., Battistelli, E. S., De Grazia, M., Luzzi, G., Orlando, A., & Savini, G. 2002, in AIP Conf. Proc. Ser. 616, Experimental Cosmology at Millimetre Wavelengths: 2K1BC Workshop, ed. M. Petris & M. Gervasi (Melville, NY: AIP), 92
 Lewis, A., & Bridle, S. 2002, *Phys. Rev. D*, **66**, 103511
 Lima, J. A. S., Silva, A. I., & Viegas, S. M. 2000, *MNRAS*, **312**, 747
 LoSecco, J. M., Mathews, G. J., & Wang, Y. 2001, *Phys. Rev. D*, **64**, 123002
 Masi, S., et al. 2003, *Mem. Soc. Astron. Ital.*, **74**, 96
 Mason, B. S., Myers, S. T., & Readhead, A. C. S. 2001, *ApJ*, **555**, L11
 Mather, J. C., Fixsen, D. J., Shafer, R. A., Mosier, C., & Wilkinson, D. T. 1999, *ApJ*, **512**, 511
 Matyjasek 1995, *Phys. Rev. D*, **51**, 4154
 Metropolis, N., Rosenbluth, A. W., Rosenbluth, M. N., Teller, A. H., & Teller, E. 1953, *J. Chem. Phys.*, **21**, 1087
 Molaro, P., Levshakov, S. A., Dessauges-Zavadsky, M., & D'Odorico, S. 2002, *A&A*, **381**, L64
 Opher, R., & Pelison, A. 2005, *MNRAS*, **362**, 167
 Overduin, J. M., & Cooperstock, F. I. 1998, *Phys. Rev. D*, **58**, 043506
 Puy, D. 2004, *A&A*, **422**, 1
 Rephaeli, Y. 1980, *ApJ*, **241**, 858
 Rephaeli, Y. 1995, *ApJ*, **445**, 33
 Savini, G., Orlando, A., Battistelli, E. S., de Petris, M., Lamagna, L., Luzzi, G., & Palladino, E. 2003, *New Astron.*, **8**, 727
 Shimon, M., & Rephaeli, Y. 2004, *New Astron.*, **9**, 69
 Srianand, R., Petitjean, P., & Ledoux, C. 2000, *Nature*, **408**, 931
 Sunyaev, R. A., & Zel'dovich, Ya. B. 1972, *Commun. Astrophys. Space Phys.*, **4**, 173
 Sunyaev, R. A., & Zel'dovich, Ya. B. 1980, *MNRAS*, **190**, 413
 Verde, L. 2007, arXiv:0712.3028
 Zemcov, M., Borys, C., Halpern, M., Mauskopf, P., & Scott, D. 2007, *MNRAS*, **376**, 1073